

1
2
3
4
5
6
7
8
9
10
11
12
13
14
15
16
17
18
19

This is a non-peer reviewed preprint submitted to EarthArXiv.

20
21
22
23
24
25
26
27
28
29
30
31
32
33
34
35
36
37
38
39
40
41

Two Pixel Reference Algorithm

Ziheng Sun¹, Liping Di¹, Hui Fang¹

zsun@gmu.edu; ldi@gmu.edu (corresponding author); hfang1288@gmail.com

¹ Center for Spatial Information Science and Systems (CSISS)

George Mason University

4087 University Dr STE 3100

Fairfax, VA, USA

Abstract: Object based image analysis (OBIA) has a unique process requirement: relate all the pixels in the segmented images to the vectorized polygons (pixel in polygon). The existing solutions are very slow in finding the pixels in a polygon. This paper proposes a novel algorithm called Two-Pixel-Reference to speed up the process. The algorithm is initially designed for segmented remote sensing images. It avoids most multiple-layer loops in existing methods and trims many redundant comparison among pixels. Thus it has literal lower Big O algorithm complexity. We implemented the algorithms in C++ and made more than seventy tests on two different machines to compare the algorithm with three other existing algorithms. The results show that it significantly decreases the time cost of the process. In every single test, the proposed algorithm costs much less time than other algorithms. Specifically, the average duration is reduced from 3.96 seconds to 0.15 second on machine #1 and from 3.647 seconds to 0.073 second on machine #2. This paper makes a good example for researching time-efficient algorithms to accelerate the overall process of OBIA in such a big data era.

42

43 **Keywords:** object based image analysis; pixel in polygon; complexity; remote sensing; image

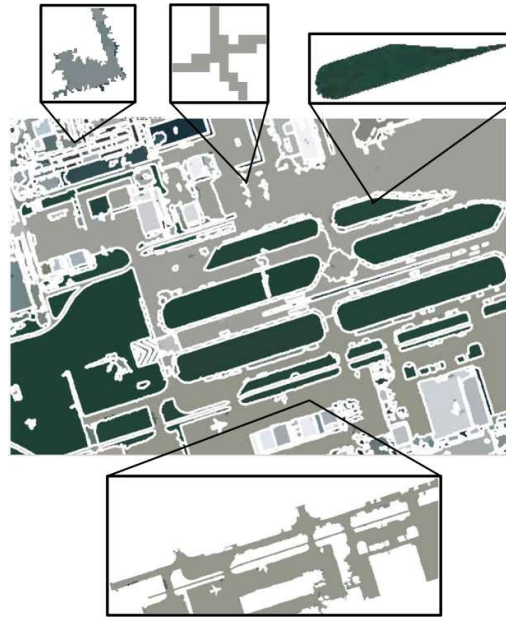
44 classification; vectorization.

45

46

47 **1. Introduction**

48 Object based image analysis (OBIA) is one of the state-of-the-art techniques in RS [1-6].
49 It first segments an image into objects, which are also called patches, segments or regions.
50 Then the post processes are conducted on the objects rather than pixels (as shown in Fig. 1).
51 Many study cases have proven that OBIA is more advantageous on enhancing the
52 classification accuracy than pixel based image analysis (PBIA) [7-10]. However, due to the
53 new object layer, OBIA has more steps than PBIA and the overall time cost of OBIA is
54 generally higher. More efforts on speeding up OBIA are needed to increase the time value of
55 OBIA results.



56

57 Figure 1. A segmented RS image and some sample segments

58 According to our experiences in building and using OBIA system [3, 11], a large block of
59 time of an OBIA analysis is spent on sorting pixels in each region after an image is segmented.
60 The existing methods have high time complexity and are very inefficient for time saving
61 purpose. Thus, this paper proposes a new algorithm of sorting pixels to decrease the duration

62 into a senseless level. The algorithm avoids most multiple-layer loops in existing methods and
63 trims many redundant comparison among pixels. Finally it evolves into an extremely concise
64 method with very low time complexity.

65 To test the algorithm, we compared four algorithms, including three existing algorithms,
66 on two machines. The inputs include an image and a vector containing polygons generated
67 from the image by raster-to-vector conversion. The output is an image, in which each pixel
68 value is set as the identifier of the vector feature the pixel belongs to. In all the experiments,
69 the input files and the output files are exactly the same. The only difference is the duration of
70 algorithm execution. We recorded the execution time and made an analysis. The results show
71 that the proposed algorithm significantly decrease the time cost. Specifically, the average
72 duration is reduced from 3.96 seconds to 0.15 second on machine #1 and from 3.647 seconds
73 to 0.073 second on machine #2.

74 The remainder of this paper is organized as follows. Section 2 introduces the background
75 knowledge. Section 3 details the new algorithm and three existing algorithms. In section 4 the
76 experiments are described and the results are evaluated. Section 5 discusses our original
77 contribution to the community. Section 6 concludes the paper and gives the future work.

78 **2. Background**

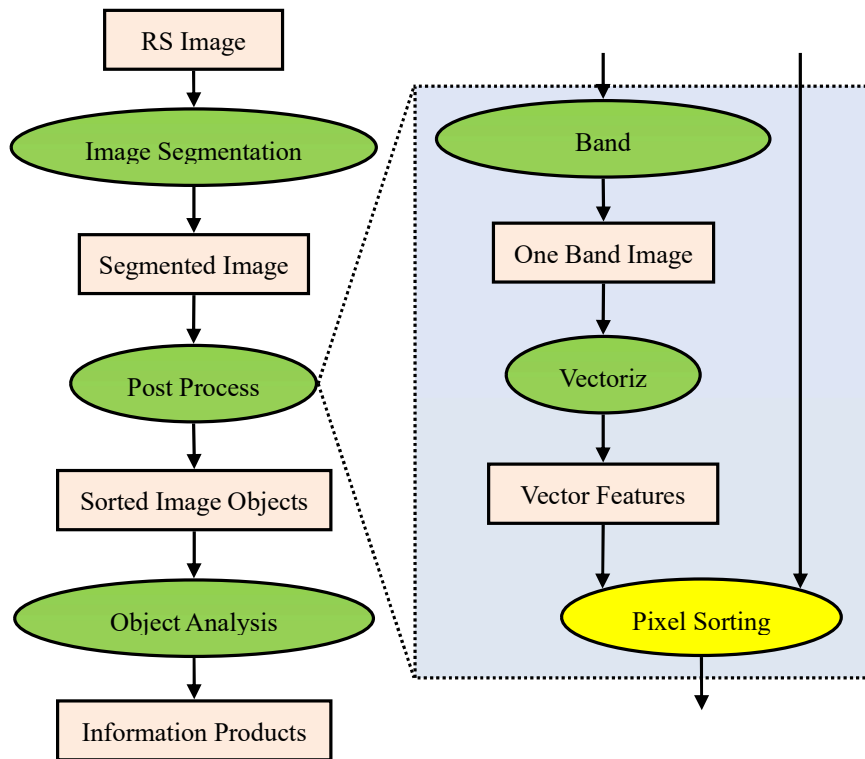
79 A large amount of RS data has been obtained by satellite-based or in-situ (e.g., airborne)
80 sensors in the last few decades. Today the amount is still aggressively growing [12, 13]. For
81 example, the NASA Earth Observing System Data and Information System (EOSDIS) [14]
82 has archived over 3.5 million individual Landsat scenes totaling around 1 petabyte of imagery
83 [15, 16]. There are many other RS products and data archive centers around the world.

84 Comparing to the speed of obtaining RS images, the speed of processing and analyzing
85 images is relatively slow [17, 18]. The complexity of applied algorithms, especially time
86 complexity, has big influences on the speed, and certainly the time value of the information
87 extracted from RS images [19]. Lowering algorithm complexity can reduce the time cost of
88 image analysis and enhance our capability of timely discovering valuable information within
89 the huge RS data.

90 OBIA, one of the current researched hot topics in RS, is comprised of three major steps:
91 image segmentation, post process and object analysis [20] (as shown in Fig. 2). Each step has
92 a set of algorithm choices. Image segmentation filters RS images into a collection of regions
93 [21]. The pixels in one region have the same value. The algorithms for this step have k-means
94 [22], ISODATA [23], mean shift [24], etc. The segmented image goes through a post process
95 including band combination, vectorizing and pixel sorting. The band combination process
96 merges all the bands into only one band. To ensure the mappings between image objects and
97 vector features are bijection, the combination should be reversible which means the one band
98 can be decomposed back to the original bands. The one band is then vectorized into a vector
99 file which outlines the image objects with polygons. Each polygon is managed as a vector
100 feature in geographic information systems. A sorting process will take the segmented image
101 and the vector features as inputs, figure out the containing relationships between the vector
102 features and the image pixels and output a image in which each pixel's value is set as the
103 identifier of the feature it belongs to (Fig. 3).

104 The post process is essential for the next process in the third step such as calculating the
105 properties of image objects. The properties of image objects have three major categories:

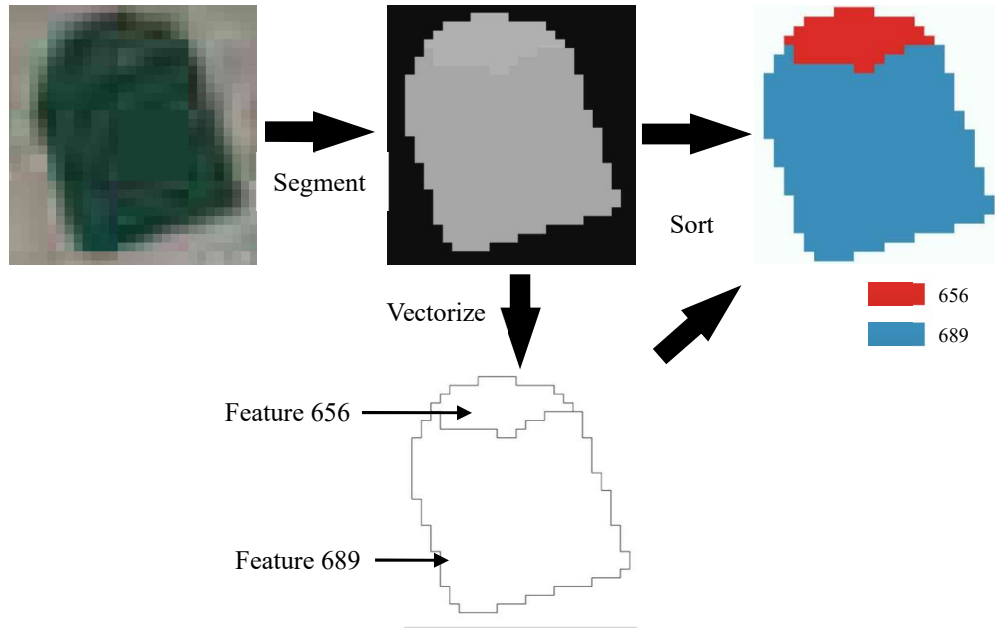
106 spatial, spectral and texture [25-27]. The spectral and texture properties of a feature are
107 calculated based on the original values of the contained pixels. Once the property values are
108 generated, people will be able to do some object analysis on them, e.g., supervised
109 classification or feature extraction (buildings, rivers, roads, forests, lakes, lawns, planes, etc)
110 [28-30].



111

112

Figure 2. The workflow of OBIA



113

114

Figure 3. Sorting pixels located in vectorized polygons

115 **3. Algorithms**

116 This section will first list three existing algorithms as comparison and then introduce a
 117 new algorithm called two-pixel-reference algorithm. All the algorithms are able to complete
 118 the pixel sorting task. But their algorithm complexity is different.

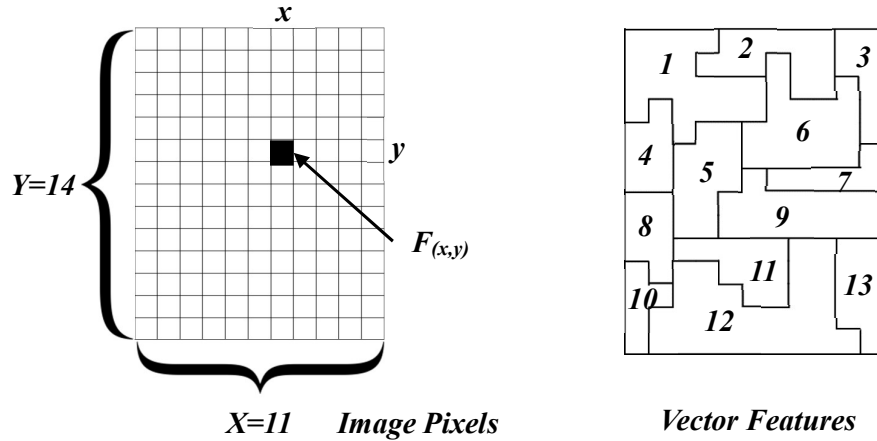
119 **3.1 Shared parameters and variables**

120 Given the inputted image is a one-band image containing X columns and Y rows of pixels.

121 The value of the pixel at column x and row y is represented by function $F_{(x,y)}$. The value of
 122 variable x ranges from 1 to X . The value of variable y ranges from 1 to Y . The corresponding

123 inputted vector file has M features/polygons whose identifiers are assigned in sequence from

124 1 to M . The features are represented by VF .



125

126

Figure 4. Example inputted image and vector parameters and variables

127 3.2 Existing algorithms

128 1) *Algorithm #1*: This algorithm is based on the widely used four direction seed spreading

129 algorithm. The basic idea is finding a pixel located in a feature and adding it as a seed into a

130 list. Then iterate all its neighbor pixels to find if there is any pixels belonging to the same

131 feature. Four direction means only the pixels located on the east, west, south and north are

132 considered as neighbor pixels. If a neighbor pixel is identified within the feature, it will be

133 taken as a new seed and added to the list. The spreading process is repeated on the new seeds

134 until all the pixels in the list have been processed. Finally, the list will contain all the pixels

135 within the feature. The core steps of this algorithm are detailed below.

-
1. Get the first seed pixel SP_i for each feature f_i in VF .
 2. For each feature f_i , add its seed SP_i to list L .
 3. Compare SP_i with its four neighbors. If a neighbor has the same value with the seed, add it to L . After all the neighbors are compared, mark SP_i as checked.
 4. Repeat Step 3 on the unchecked seed in L until all the seeds in L are checked. The pixels in
-

L will be the pixels contained in f_i .

5. Repeat Step 1~4 to sort all the features in VF .

136 Because the deepest step (Step 3) in the loops could be run by up to $M \times (X \times Y)^4$ times,
137 the Big-O complexity of this algorithm is:

138
$$T_{algorithm1} = O_{(M \times (X \times Y)^4)}$$

139 M is not a constant variable so it can NOT be ignored.

140 2) *Algorithm #2*: This algorithm is an improved version of algorithm #1. It takes advantage of
141 a characteristics of the segmented image. If the first seed's pixel value of a feature is unique
142 among the first seeds of all the features, then all the pixels with this value directly belongs to
143 the feature. The steps of algorithm #2 are:

1. Get the first seed pixels for all the features in VF .
 2. If the first seed pixel value of f_i is unique, find all the pixels with this value and belong them to f_i .
 3. For those features whose first seed pixel values are not unique, apply Algorithm #1.
-

144 Suppose the number of the features having unique first seed pixel values is K , then the
145 complexity of algorithm #2 is:

146
$$T_{algorithm} = O_{((M-K) \times (X \times Y)^4)}$$

147 3) *Algorithm #3*: This algorithm is a mutation of algorithm #1. Algorithm #1 and #2 stand on
148 the position of features, while this algorithm is in the perspective of pixels. The steps are
149 described below.

1. Get the first seed pixels for all the features in VF . Add them to a list L_I .
 2. All the pixels are initially marked as unchecked. Scan the pixels line by line.
-

-
3. For each unchecked pixel $P(x, y)$, use it as a seed and apply Algorithm #1 to get a list of pixels L_2 .
 4. Search L_1 to get the first seed which is listed in L_2 . Get the feature corresponding to the seed. Belong L_2 to the feature.
 5. Mark all the pixels in L_2 as checked.
 6. Repeat 3~5 until all the pixels in the image are checked.
-

150 The complexity of this algorithm is:

151
$$T_{algorithm3} = O((X \times Y)^4)$$

152 **3.3 Two-Pixel-Reference (TPR) Algorithm**

153 This algorithm avoids most loops in the above three algorithms and trims redundant
 154 comparison among pixels to speed up the process. It fully takes advantage of the boundaries
 155 of vector features and uses two direction comparison to prevent duplicated comparison. Only
 156 three steps are performed in this algorithm. In each step, the loop has no more than two layers
 157 to ensure the complexity stays low. The steps are detailed below.

1. For each feature f_i in \mathcal{VF} , mark the pixels adjacent to its boundary and locating within f_i by f_i 's identifier. Repeat this step until all the pixels adjacent to feature boundaries are marked.
 2. Scan the image row by row. If a pixel $P_{(x, y)}$ is not marked, compare its value $F_{(x, y)}$ with $F_{(x-1, y)}$ and $F_{(x, y-1)}$. If equal to one of them, mark P with the equal one's feature identifier. Repeat this step until all the pixels are marked.
 3. Set the identifier values to corresponding pixels and output the image.
-

158 This algorithm will be referred to as Algorithm #4 hereafter in this paper. The complexity
 159 of this algorithm is:

160
$$O_{algorithm4} = O_{(X \times Y)}$$

161 According to the Big O algorithm complexity rules [31, 32], The four algorithms are
162 placed in order from high complexity to low complexity as:

163
$$O_{algorithm1} > O_{algorithm2} > O_{algorithm3} > O_{algorithm4}$$

164 Therefore, TPR algorithm has the lowest algorithm complexity literally. Next section will
165 test the physical influences on time cost through experiments.

166 **4. Implementation, Experiment and Results**

167 We implement the four algorithms using C++ language with support from GDAL library
168 [33]. The code is available in a public GitHub repository
169 <https://github.com/VirginiaJRS/PixelsInSegment>.

170 We run the code on a test image on two machines. Fig. 5a shows the original test image,
171 a high resolution optical remote sensing image of the Dallas Love Field Airport at Texas, U.S.
172 Fig. 5b and 5c are the input files of the algorithms and Fig. 5d is the outputted image. One test
173 machine is a HP laptop with Windows 7 64-bit system, Intel Core i5-2450M CPU (2.50GHz)
174 and 6 gigabytes RAM memory. The other machine is a HP Proliant DL180 G6 rack server
175 with Ubuntu Linux 12.04 LTS system, 8 core Intel(R) Xeon(R) CPU E5606 (2.13GHz) and 8
176 gigabytes RAM memory.

177 As the operating systems are in parallel processing mode, other running threads at the
178 same time will definitely impact the duration of each execution of the algorithms. To reduce
179 the uncertain impacts of the external factors and create a fair test environment, we killed as
180 many threads as possible before the tests are conducted. During the test, both machines are
181 dedicated and not be used for any other tasks. The execution time is automatically recorded

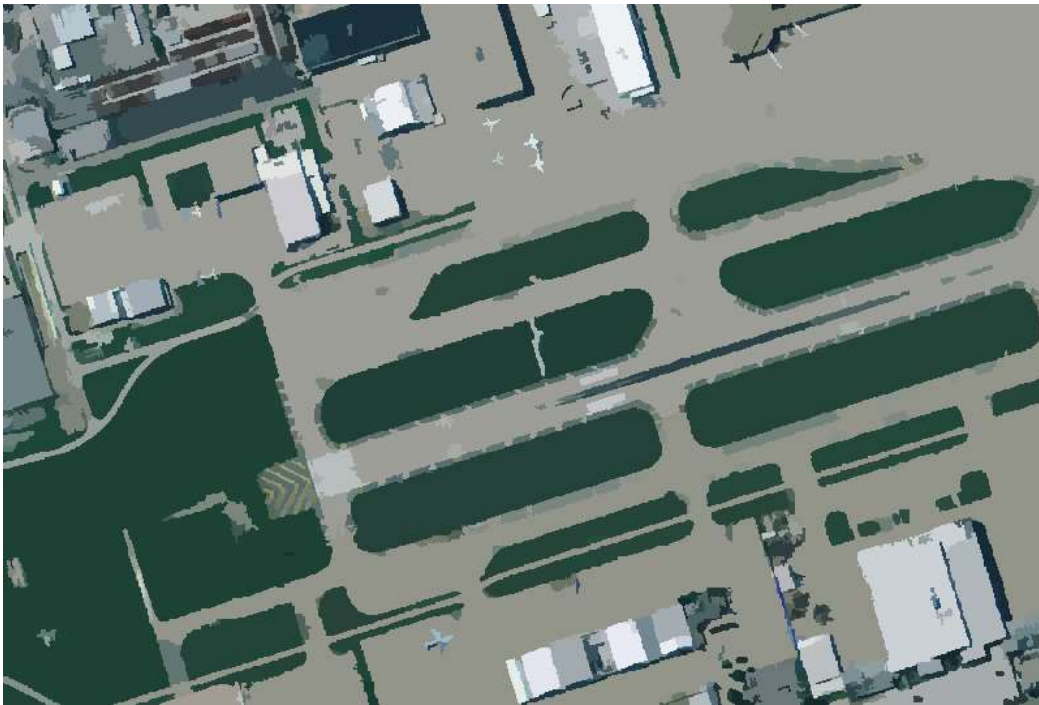
182 by the code and exported to tables by a Shell script. We visualized the time cost data into
183 multiple plots as shown in Fig. 6.



184

(a)

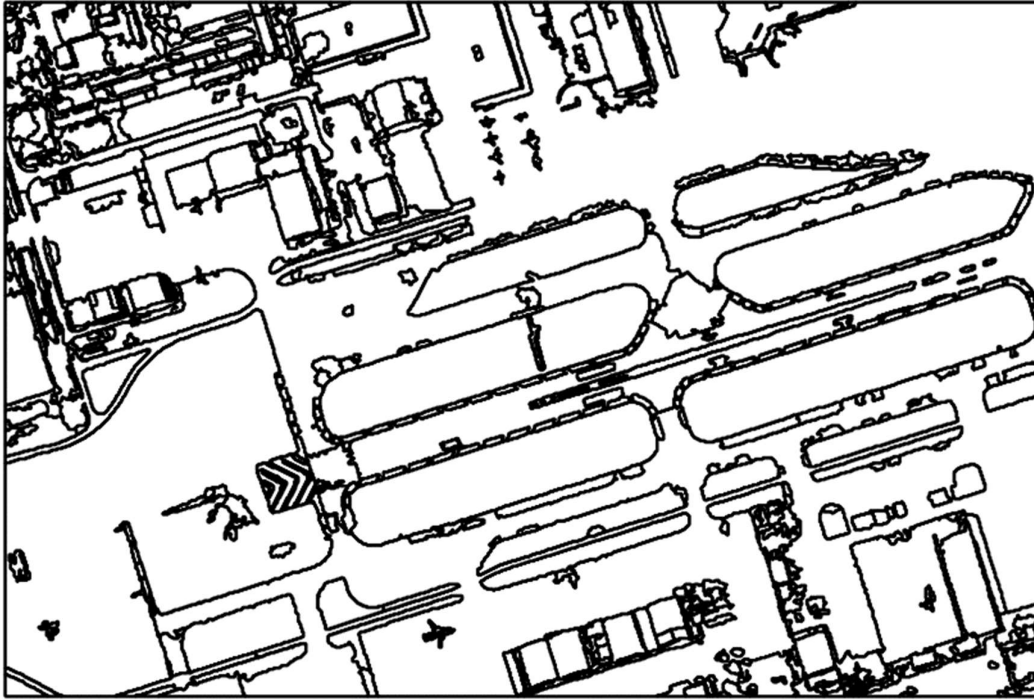
185



186

(b)

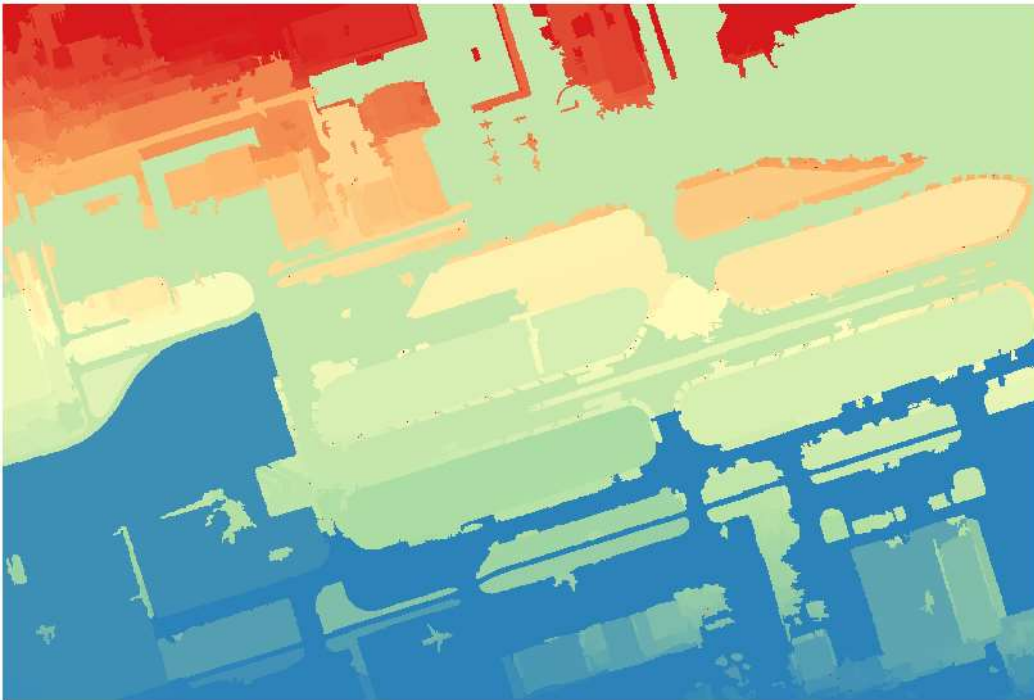
187



188

189

(c)



190

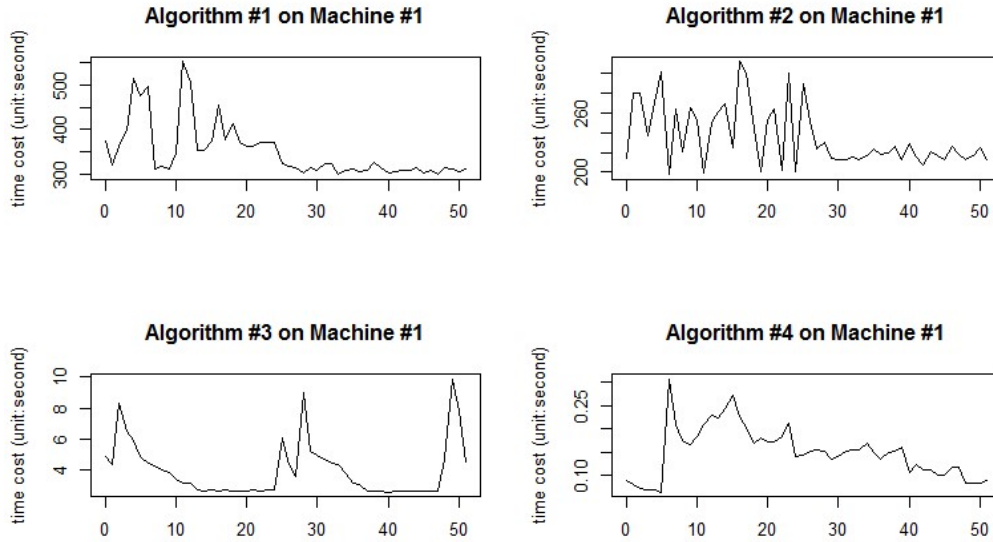
191

(d)

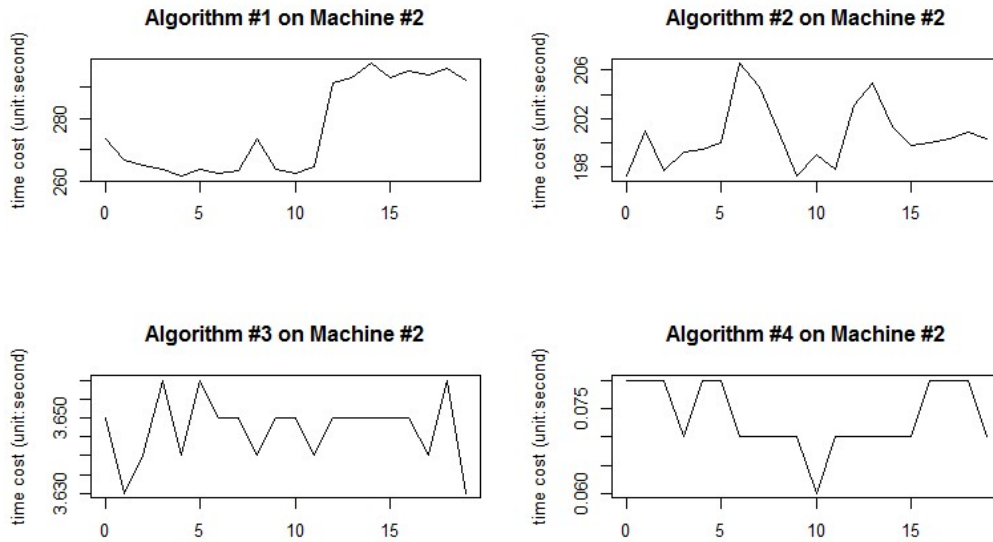
192 Figure 5. The inputs and output of the test image. (a) original image; (b) segmented image; (c)

193

vector file; (d) pixel-sorted image



194



195

196

Figure 6. The time costs of four algorithms on two machines

197

In Fig. 6, overall fifty tests are recorded on machine #1 and twenty tests are recorded on

198

#2. Although we tried to make a clean test environment, the time cost still varies largely for

199

the same algorithm. For example, the time cost of Algorithm #1 on machine #1 ranges from

200 300 seconds to 550 seconds, while the time cost on machine #2 ranges from 260 seconds to
 201 300 seconds. Generally for all the four algorithms, the time cost on machine #2, which is a
 202 rack server, is more stable than machine #1 which is a laptop. But the differences on time cost
 203 among algorithms are still very apparent. The range of time cost of the four algorithms is
 204 listed in Table 1. All the ranges are never overlapped with each other and have a clear
 205 high-to-low sequence which completely agrees with the literal order analyzed in Section 3.
 206 The time cost of the TPR algorithm (#4) is obviously the lowest on both machines. We also
 207 calculated the average time cost of each algorithm on the two machines (Table 2). The time
 208 cost of algorithm #4 is always below 0.2 second. Such an interval is actually senseless by
 209 human beings. Comparing to the time cost of 3 seconds (algorithm #3), 200 seconds
 210 (algorithm #2) and 270 seconds (algorithm #1), TPR algorithm significantly compressed the
 211 time cost of this process into a very satisfying level.

212 The dimension of the test image is 800 pixels (X) by 538 pixels (Y) and the number of
 213 features is 900 (M). If the inputted image is changed to a larger one and the feature number
 214 also increases, the time cost of each algorithm will definitely increase. According to the
 215 Big-O algorithm complexity rules, the time cost of algorithm #4 will remain the lowest
 216 among the four.

217 Table 1. The ranges of time cost for the four algorithms (unit: second)

	Algorithm #1	Algorithm #2	Algorithm #3	Algorithm #4
Machine #1	300~550	200~280	2~10	0.07~0.3
Machine #2	260~300	197~207	3.63~3.66	0.06~0.08

218 Table 2. The average time costs of the four algorithms on two machines (unit: second)

	Algorithm #1	Algorithm #2	Algorithm #3	Algorithm #4
Machine #1	350.321	235.810	3.96	0.15
Machine #2	276.823	200.578	3.647	0.073

219 **5. Discussion**

220 5.1 Performance

221 TPR algorithm can help speed up the process of OBIA and shorten the interval between
222 the image acquired date and the image analyzed date. A direct impact on service providers
223 and endpoint users is the data processing time is reduced. There are three major modes for RS
224 image analysis: manual, semi-automatic and automatic. The semi-automatic mode allows
225 image analysts to use GIS/RS software such as ArcGIS, ENVI, ERDAS, eCognition for
226 automatic assistance and is the most used one. The workflow is sequential. Once an analyst
227 submits a request to the systems, (s) he will have to wait until the segmentation is completed.
228 If one process like the pixel sorting process becomes faster, the time that analyzers spend on
229 waiting will decrease respectively. The time for analyzing an image will lower too. Eventually
230 the interval between the image acquiring date and the date when endpoint users receive the
231 analyzed products will shrink. This is very meaningful in urgent cases such as earthquake,
232 flooding, wild fire, debris flow and typhoon when every second counts.

233 5.2 Application Vision

234 This algorithm provides a good example for researchers to develop optimal complexity
235 algorithms for time saving purposes. Most current researchers in RS mainly focus on
236 improving result accuracy and show less care on time costs. In many researches, the
237 efficiency of algorithms is sacrificed to pursue for a more accurate result such as Neural

238 Network and SVM based image analysis techniques. Their outputs may have higher accuracy
239 but take much longer than basic analysis techniques. In other words, more recent researches
240 are engaged in augmenting the information value of RS products but ignore the time value.
241 This work try to display the power of time-efficient algorithms in RS and make the overall
242 duration of an analysis on a RS image into an endurable level.

243 **6. Conclusion and Future Work**

244 This paper proposes a novel algorithm, named TPR algorithm, to speed up the process of
245 sorting pixels in segmented RS images. It avoids most multiple-layer loops in existing
246 methods and trims many redundant comparison among pixels. It fully leverages the
247 boundaries of vector features and uses two direction comparison to prevent duplicated
248 comparison. Its Big O algorithm complexity is very lower than existing algorithms. We
249 implemented the algorithm in C++ and published the code onto GitHub. Experiments have
250 been made by running the code with a high resolution optical RS test image on two different
251 machines. In every single test, the time cost of TPR algorithm is always the lowest. The
252 results prove that the new algorithm significantly decreases the time cost of the process. The
253 average duration is reduced from 3.96 seconds to 0.15 second on machine #1 and from 3.647
254 seconds to 0.073 second on machine #2. The algorithm sets a good example for time-efficient
255 algorithms to speed up the overall process of OBIA in the big data era.

256 To make TPR algorithm able to serve as a robust building block in OBIA, we will
257 maintain and update the code on GitHub. Besides, the current test image is a high resolution
258 optical image. We will apply the algorithm on high spectral images in our next stage of work.
259 In addition, how to fasten the other steps in OBIA while keeping the accuracy not going down

260 will be studied too.

261

262

263

264 **Reference**

- 265 1 Blaschke, T.: ‘Object based image analysis for remote sensing’, ISPRS Journal of
266 Photogrammetry and Remote Sensing, 2010, 65, (1), pp. 2-16
- 267 2 Di, L., Yue, P., and Sun, Z.: ‘Ontology-supported complex feature discovery in a web
268 service environment’, in Editor (Ed.)^(Eds.): ‘Book Ontology-supported complex feature
269 discovery in a web service environment’ (2012, edn.), pp. 2887-2890
- 270 3 Sun, Z., Fang, H., Di, L., Yue, P., Tan, X., and Bai, Y.: ‘Developing a web-based system
271 for supervised classification of remote sensing images’, GeoInformatica, 2016, pp. 1-21
- 272 4 Sun, Z., Di, L., Chen, A., Yue, P., and Gong, J.: ‘The use of geospatial workflows to
273 support automatic detection of complex geospatial features from high resolution images’, in
274 Editor (Ed.)^(Eds.): ‘Book The use of geospatial workflows to support automatic detection of
275 complex geospatial features from high resolution images’ (IEEE, 2013, edn.), pp. 159-162
- 276 5 Sun, Z., Di, L., and Fang, H.: ‘Using long short-term memory recurrent neural network
277 in land cover classification on Landsat and Cropland data layer time series’, International
278 Journal of Remote Sensing, 2018, 40, (2), pp. 593-614
- 279 6 Sun, Z., Di, L., Fang, H., Burgess, A.B., and Singh, N.: ‘Deep Learning
280 Cyberinfrastructure for Crop Semantic Segmentation’, in Editor (Ed.)^(Eds.): ‘Book Deep
281 Learning Cyberinfrastructure for Crop Semantic Segmentation’ (AGU, 2019, edn.), pp.
- 282 7 Duro, D.C., Franklin, S.E., and Dubé, M.G.: ‘A comparison of pixel-based and
283 object-based image analysis with selected machine learning algorithms for the classification
284 of agricultural landscapes using SPOT-5 HRG imagery’, Remote Sensing of Environment,
285 2012, 118, pp. 259-272
- 286 8 Blaschke, T., Hay, G.J., Kelly, M., Lang, S., Hofmann, P., Addink, E., Queiroz Feitosa,
287 R., van der Meer, F., van der Werff, H., van Coillie, F., and Tiede, D.: ‘Geographic
288 Object-Based Image Analysis – Towards a new paradigm’, ISPRS Journal of Photogrammetry
289 and Remote Sensing, 2014, 87, pp. 180-191
- 290 9 Benarchid O., Raissouni N., El Adib S., Abbous A., Azyat A., Ben Achhab N., Lahraoua
291 M. , and A., C.: ‘Building Extraction using Object-Based Classification and Shadow
292 Information in Very High Resolution Multispectral Images, a Case Study: Tetuan, Morocco’,
293 Canadian Journal on Image Processing and Computer Vision, 2013, 4, (1), pp. 1-8
- 294 10 Hussain, M., Chen, D., Cheng, A., Wei, H., and Stanley, D.: ‘Change detection from
295 remotely sensed images: From pixel-based to object-based approaches’, ISPRS Journal of
296 Photogrammetry and Remote Sensing, 2013, 80, pp. 91-106
- 297 11 Sun, Z., Fang, H., Deng, M., Chen, A., Yue, P., and Di, L.: ‘Regular Shape Similarity
298 Index: A Novel Index for Accurate Extraction of Regular Objects from Remote Sensing
299 Images’, Geoscience and Remote Sensing, IEEE Transactions on, 2015, 53, (7), pp.
300 3737-3748
- 301 12 Heipke, C., Madden, M., Li, Z., and Dowman, I.: ‘Theme issue “State-of-the-art in
302 photogrammetry, remote sensing and spatial information science”’, ISPRS Journal of
303 Photogrammetry and Remote Sensing, 2016, (115), pp. 1-2
- 304 13 Chi, M., Plaza, A.J., Benediktsson, J.A., Zhang, B., and Huang, B.: ‘Foreword to the
305 Special Issue on Big Data in Remote Sensing’, Selected Topics in Applied Earth Observations
306 and Remote Sensing, IEEE Journal of, 2015, 8, (10), pp. 4607-4609

307 14 <https://earthdata.nasa.gov/about>, accessed 2016.5.16
308 15 http://landsat.usgs.gov/Landsat_Project_Statistics.php, accessed 2014.9.21
309 16
310 <https://hyspeedblog.wordpress.com/2013/03/22/big-data-and-remote-sensing-where-does-all-this-imagery-fit-into-the-picture/>, accessed 2016.5.16
311
312 17 Ma, Y., Wu, H., Wang, L., Huang, B., Ranjan, R., Zomaya, A., and Jie, W.: 'Remote
313 sensing big data computing: Challenges and opportunities', *Future Generation Computer*
314 *Systems*, 2015, 51, pp. 47-60
315 18 Li, S., Dragicevic, S., Castro, F.A., Sester, M., Winter, S., Coltekin, A., Pettit, C., Jiang,
316 B., Haworth, J., Stein, A., and Cheng, T.: 'Geospatial big data handling theory and methods: A
317 review and research challenges', *ISPRS Journal of Photogrammetry and Remote Sensing*,
318 2016, 115, pp. 119-133
319 19 Rathore, M.M.U., Paul, A., Ahmad, A., Chen, B.W., Huang, B., and Ji, W.: 'Real-Time
320 Big Data Analytical Architecture for Remote Sensing Application', *IEEE Journal of Selected*
321 *Topics in Applied Earth Observations and Remote Sensing*, 2015, 8, (10), pp. 4610-4621
322 20 Hay, G.J., and Castilla, G.: 'Geographic Object-Based Image Analysis (GEOBIA): A new
323 name for a new discipline': 'Object-based image analysis' (Springer, 2008), pp. 75-89
324 21 Shi, J., and Malik, J.: 'Normalized cuts and image segmentation', *Pattern Analysis and*
325 *Machine Intelligence, IEEE Transactions on*, 2000, 22, (8), pp. 888-905
326 22 Ahmad, A., and Dey, L.: 'A k-mean clustering algorithm for mixed numeric and
327 categorical data', *Data & Knowledge Engineering*, 2007, 63, (2), pp. 503-527
328 23 Ball, G.H., and Hall, D.J.: 'ISODATA, a novel method of data analysis and pattern
329 classification', in Editor (Ed.)^(Eds.): 'Book ISODATA, a novel method of data analysis and
330 pattern classification' (DTIC Document, 1965, edn.), pp.
331 24 Comaniciu, D., and Meer, P.: 'Mean shift: A robust approach toward feature space
332 analysis', *Pattern Analysis and Machine Intelligence, IEEE Transactions on*, 2002, 24, (5), pp.
333 603-619
334 25 Fauvel, M., Benediktsson, J.A., Chanussot, J., and Sveinsson, J.R.: 'Spectral and spatial
335 classification of hyperspectral data using SVMs and morphological profiles', *Geoscience and*
336 *Remote Sensing, IEEE Transactions on*, 2008, 46, (11), pp. 3804-3814
337 26 Manjunath, B.S., and Ma, W.-Y.: 'Texture features for browsing and retrieval of image
338 data', *Pattern Analysis and Machine Intelligence, IEEE Transactions on*, 1996, 18, (8), pp.
339 837-842
340 27 He, D.-C., and Wang, L.: 'Texture features based on texture spectrum', *Pattern*
341 *Recognition*, 1991, 24, (5), pp. 391-399
342 28 Yan, J., Lin, L., Zhou, W., Ma, K., and Pickett, S.T.: 'A novel approach for quantifying
343 particulate matter distribution on leaf surface by combining SEM and object-based image
344 analysis', *Remote Sensing of Environment*, 2016, 173, pp. 156-161
345 29 Shirke, S., Pinto, S.M., Kushwaha, V.K., Mardikar, T., and Vijay, R.: 'Object-based
346 image analysis for the impact of sewage pollution in Malad Creek, Mumbai, India',
347 *Environmental Monitoring and Assessment*, 2016, 188, (2), pp. 1-12
348 30 Yan, M., Blaschke, T., Tang, H., Xiao, C., Sun, X., Zhang, D., and Fu, K.: 'Using
349 object-based analysis to derive surface complexity information for improved filtering of
350 airborne laser scanning data', *Frontiers of Earth Science*, 2016, pp. 1-9

351 31 Papadimitriou, C.H.: ‘Computational complexity’ (John Wiley and Sons Ltd., 2003.
352 2003)
353 32 Papadimitriou, C.H., and Steiglitz, K.: ‘Combinatorial optimization: algorithms and
354 complexity’ (Courier Corporation, 1982. 1982)
355 33 <http://www.gdal.org>, accessed Mar 20 2015

356

357

358 Figures

359 Figure 1. A segmented RS image and some sample segments

360 Figure 2. The workflow of OBIA

361 Figure 3. Sorting pixels located in vectorized polygons

362 Figure 4. Example inputted image and vector parameters and variables

363 Figure 5. The inputs and output of the test image. (a) original image; (b) segmented image; (c)
364 vector file; (d) pixel-sorted image

365 Figure 6. The time costs of four algorithms on two machines

366

367

368 Tables

369 Table 1. The ranges of time cost for the four algorithms (unit: second)

370 Table 2. The average time costs of the four algorithms on two machines (unit: second)

371